AIAA 2000-1045
A Multidisciplinary Performance Analysis of a Lifting-Body Single-Stage-to-Orbit Vehicle

Paul V. Tartabini
Roger A. Lepsch
J. J. Korte
Kathryn E. Wurster
NASA Langley Research Center
Hampton, VA 23681-2199

38th Aerospace Sciences Meeting & Exhibit
10-13 January 2000 / Reno, NV

AIAA-2000-1045

A MULTIDISCIPLINARY PERFORMANCE ANALYSIS OF A LIFTING-BODY SINGLE-STAGE-TO-ORBIT VEHICLE

Paul V. Tartabini[*], Roger A. Lepsch[†], J. J. Korte[‡] and Kathryn E. Wurster[§]
NASA Langley Research Center
Hampton, Virginia 23681

ABSTRACT

Lockheed Martin Skunk Works (LMSW) is currently developing a single-stage-to-orbit reusable launch vehicle called VentureStar™. A team at NASA Langley Research Center participated with LMSW in the screening and evaluation of a number of early VentureStar™ configurations. The performance analyses that supported these initial studies were conducted to assess the effect of a lifting body shape, linear aerospike engine and metallic thermal protection system (TPS) on the weight and performance of the vehicle. These performance studies were performed in a multidisciplinary fashion that indirectly linked the trajectory optimization with weight estimation and aerothermal analysis tools. This approach was necessary to develop optimized ascent and entry trajectories that met all vehicle design constraints.

Significant improvements in ascent performance were achieved when the vehicle flew a lifting trajectory and varied the engine mixture ratio during flight. Also, a considerable reduction in empty weight was possible by adjusting the total oxidizer-to-fuel and liftoff thrust-to-weight ratios. However, the optimal ascent flight profile had to be altered to ensure that the vehicle could be trimmed in pitch using only the flow diverting capability of the aerospike engine. Likewise, the optimal entry trajectory had to be tailored to meet TPS heating rate and transition constraints while satisfying a crossrange requirement.

NOMENCLATURE

cg	Center-of-gravity
C_L	Lift coefficient
GLOW	Gross Lift-off Weight, klbs
I_{SP}	Specific Impulse, sec
LaRC	NASA Langley Research Center
LH_2	Liquid Hydrogen
LMSW	Lockheed Martin Skunk Works
LOX	Liquid Oxygen
MECO	Main Engine Cut Off
M_e	Edge Mach Number
M_∞	Freestream Mach Number
O/F	Total oxidizer-to-fuel ratio
q	Dynamic pressure, psf
q-α	Dynamic pressure times angle-of-attack, psf-deg
Re_θ	Momentum Thickness Reynolds Number
RLV	Reusable Launch Vehicle
S	Aerodynamic reference area, ft^2
T/W	Thrust-to-weight ratio
$(T/W)_{eng}$	Engine thrust-to-weight ratio
TVC	Thrust Vector Control
W	Entry weight, lbs
W_{empty}	Empty weight, lbs
W_{ins}	Inserted weight, lbs
X/L	Body position over vehicle length
α	Angle-of-attack, deg
Δ payload	Change in payload from baseline

INTRODUCTION

Many papers have been written describing the difficulty of designing a fully reusable single-stage-to-orbit launch vehicle.[1-3] The physical difficulty of this problem is further exacerbated by the large degree of coupling between the various design disciplines. Nearly every subsystem design decision has far reaching consequences that must be evaluated in a multidisci-

Research Engineer, Mail Stop 365, Vehicle Analysis Branch.
†*Senior Research Engineer, Mail Stop 365, Vehicle Analysis Branch, Member AIAA.*
‡*Senior Research Engineer, Mail Stop 159, Multidisciplinary Optimization Branch, Senior Member AIAA.*
§*Senior Research Engineer, Mail Stop 365, Vehicle Analysis Branch, Associate Fellow AIAA.*

¶The use of trademarks or names of manufacturers in this report is for accurate reporting and does not constitute an official endorsement, either expressed or implied, of such products or manufacturers by the National Aeronautics and Space Administration.

plinary fashion in order to assess the impact on the weight and performance of the entire vehicle. This paper discusses this process as it relates to the conceptual design and analysis of Lockheed Martin Skunk Works' (LMSW) proposed single-stage-to-orbit commercial reusable launch vehicle (RLV), VentureStar™.

LMSW is currently studying the VentureStar™ RLV which has a number of unique features that differentiate it from other SSTO concepts evaluated in the past. Chief among these differences is the lifting body shape of the vehicle and the utilization of the linear aerospike engine. These design features and others, such as the use of a metallic thermal protection system (TPS), provide numerous benefits that may ultimately contribute to a fully capable vehicle that approaches NASA's goal of enabling commercial access to space at an order of magnitude less than today's cost.[4] A representative VentureStar™ configuration is shown in Fig. 1.

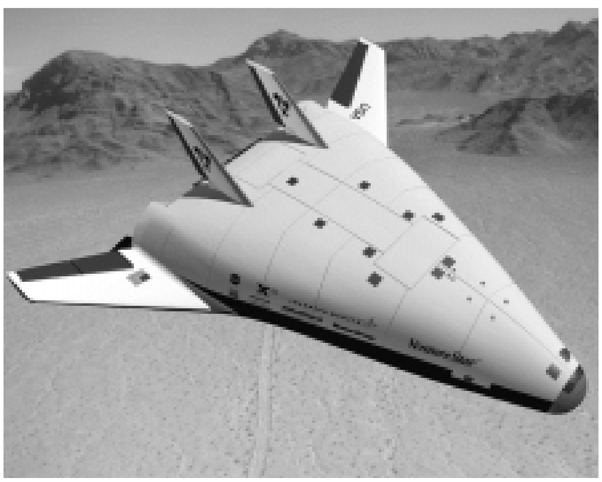

Figure 1. A representative VentureStar™ Configuration.

The decision to proceed with the full-scale development of VentureStar™ will be made upon the conclusion of the X-33 program. This program is a joint venture between NASA and LMSW and includes the design, construction, and flight testing of the X-33 in order to demonstrate technologies critical to the development of VentureStar™. In 1997, after a year of dedicated effort in the design of the X-33, LMSW began to use the lessons learned to improve the conceptual design of the full-scale VentureStar™. During this phase of the program, NASA Langley Research Center (LaRC) participated in the design, analysis and screening of a number of different vehicle concepts and configurations.[5]

Throughout the duration of the LaRC study, the feasibility of numerous configurations was evaluated in terms of vehicle mass and payload capability. These mass properties are directly related to the overall performance of the vehicle. Since many design parameters affect both weight and performance, accurate determination of vehicle sizing information requires a multidisciplinary approach to performance analysis. The approach utilized in this study indirectly coupled trajectory optimization, weight estimation, and heating analysis tools to ascertain the impact of various design options on the payload capability of each configuration. Using this approach, trade studies were conducted to maximize vehicle performance and cost effectiveness. The primary objective of these studies was to address design issues that presented opportunities and challenges that were unique to VentureStar™. Specifically, this paper addresses issues that pertain to 1) the effect of the lifting body shape and aerospike engine on ascent performance, 2) the ability to influence vehicle sizing by varying the engine size and mixture ratio, and 3) the ramifications of the metallic thermal protection system on the entry trajectory design. A multidisciplinary approach was the only way to ensure that the system fully exploited the performance benefits offered by the unique VentureStar™ design while staying within the operational limits imposed by its cost-saving elements.

APPROACH

Many of the trades discussed in this paper required the calculation of various physical characteristics of the vehicle including payload capability, empty weight and gross lift-off weight (GLOW). These quantities were predicted using a multi-disciplinary analysis that included trajectory optimization, weights and sizing estimation and engine performance prediction.

Trajectory optimization, which formed the core of this analysis method, was performed using the three-degree-of-freedom version of the Program to Optimize Simulated Trajectories (POST).[6] This program has been developed as a joint government/contractor effort, and it is available and widely used within the aerospace community. Inputs to this code include Earth atmospheric and gravitational models, system mass properties, engine performance, and vehicle aerodynamics.

Mass property estimation was conducted using the Configuration Sizing program (CONSIZ).[7] CONSIZ utilizes parametric mass-estimating relationships based on historical regression, finite element analysis and technology readiness level. With knowledge of the vehicle layout, CONSIZ can also be used to estimate the location of the vehicle center-of-gravity for trim calculations. In this paper, mass property data was generated by LaRC using CONSIZ and was calibrated to weight statements released by LMSW. Another required input to POST was a propulsion data model that was computed using a suite of computer codes that simulated linear aerospike engine performance. These codes were able to generate an aerospike engine database as a function of altitude, mixture ratio, power level and thrust vectoring for use within the POST trajectory code. The capabilities and development of these tools are discussed in Reference 8. A final input to the trajectory optimization was an aerodynamic database that included coefficients for lift, drag and pitching moment as a function of Mach number, angle-of-attack and control surface deflection. This database was obtained through the blending of solutions from computational methods and wind tunnel data. Updates to the aerodynamic coefficients were made periodically during the conceptual design phase to reflect configuration shape changes.

All of the entry performance trades discussed in this paper were performed using POST and MINIVER.[9] POST was the ideal tool to perform entry trajectory optimization, but was limited in its ability to provide heating environments. An aerothermal analysis tool, MINIVER, was chosen to complement POST and to provide a reliable measure of the heating levels during trajectory development. MINIVER is an engineering code that uses approximate heating methods with simple flowfield and geometric shapes to model heating on critical regions of the vehicle. MINIVER has been used extensively as a preliminary design tool and has demonstrated excellent agreement with more detailed heating solutions for stagnation and windward acreage areas on a wide variety of vehicle configurations.[10-12] In addition to providing sufficiently accurate heating levels, it can be used to predict the onset of transition to turbulent flow.

RESULTS AND DISCUSSION

Ascent Performance

The figure of merit used for the ascent trade studies was payload capability. This parameter was determined for each vehicle assuming a constant propellant volume, which ensured that the vehicles being compared were similar in size (dry weight), thus minimizing errors due to scaling. The design reference mission for the VentureStar™ RLV was delivery of a 25-klb payload to the International Space Station (ISS). The nominal ascent trajectory began with launch at Kennedy Space Center and ended with the insertion of the payload into a 50 × 248 nmi orbit inclined 51.6°. At this point the RLV coasted to apogee where the Orbital Maneuvering System (OMS) engines were used to circularize at the ISS altitude.

The aerospike engine performance reflected the baseline propulsion system at the conclusion of this study with 8 engines operating at a chamber pressure of 2,500 psia and an area ratio of 196. A LaRC version of this database was created that provided realistic engine performance across the mixture ratio/power level envelope, thereby minimizing the amount of interpolation error.

The nominal VentureStar™ ascent trajectory was determined by maximizing the weight inserted into the target orbit. The trajectory was optimized by adjusting the pitch attitude, engine power level and engine mixture ratio flight profiles. These control variables were constrained by angle-of-attack and engine operating limits. An additional constraint was imposed on the mixture ratio profile which had to be varied such that the ratio of oxidizer to fuel was consistent with the vehicle tank design value of 6.0. The optimized trajectory had to meet a number of inflight constraints including limits on axial acceleration, dynamic pressure, q-α, and angle of attack. The parameter q-α is proportional to the structural loading of the vehicle during flight and is the product of dynamic pressure and angle-of-attack. The nominal trajectory was untrimmed. A subsequent section will discuss the trim capability of the aerospike thrust vector control (TVC) system and the effect of a trim constraint on vehicle performance. The values of all flight constraints and control limits are listed in Table 1.

The significant flight parameter profiles for the nominal VentureStar™ ascent trajectory are shown in Figs. 2a and 2b. Main engine cut off (MECO) took place near perigee of the transfer orbit, at an altitude of 57 nmi and a flight path angle near 0.1°. The peak dynamic pressure

Table 1. Constraints imposed upon nominal ascent trajectory

Constraint Name	Constraint Value
Final Orbit	50 × 248 nmi
Final Inclination	51.6 deg
Axial Acceleration Limit	$a_x \leq 3$ g's
Dynamic Pressure Limit	$q \leq 600$ psf
q-α Limits	$\lvert q\text{-}\alpha \rvert \leq 1500$ psf
Angle-of-attack Limits	$-4 \text{ deg} \leq \alpha \leq 12 \text{ deg}$
Lift-off Thrust to Weight Ratio	1.35
Overall Tank Ratio	6.0
Engine Power Level	0.2 ≤ power level ≤ 1.0
Engine Mixture Ratio	5.5 ≤ mixture ratio ≤ 7.0

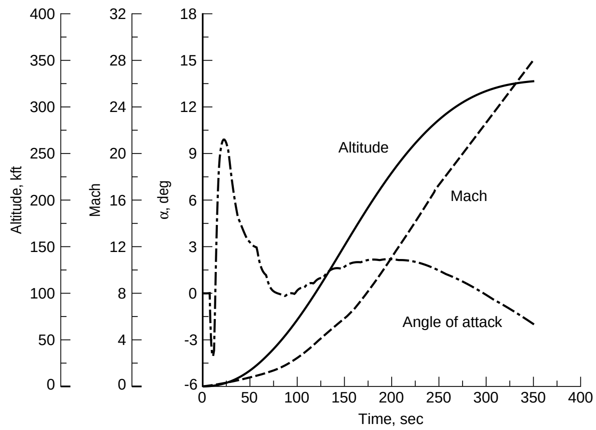

a. Altitude, Mach, and angle-of-attack profiles.

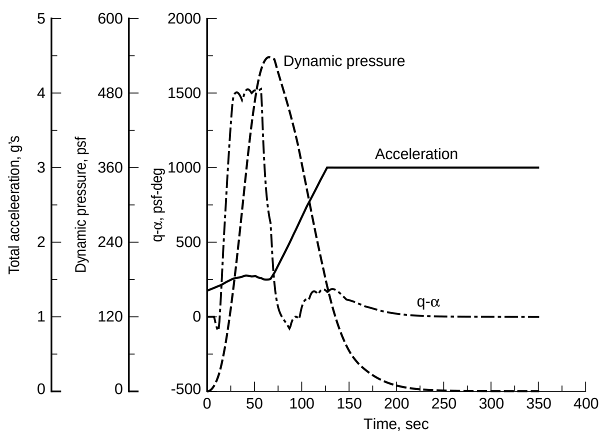

b. Acceleration, dynamic pressure, and q-α profiles.

Figure 2. Important flight parameter profiles for the nominal ascent trajectory.

of 540 psf occurred at a Mach number of 1.1 and the q-α limit of 1500 psf-deg was held for roughly 25 sec. from Mach 0.4 to 0.6. Although these two structural parameters were kept within their required limits throughout the trajectory, the peak normal force was nearly 2.3 times the empty weight of the vehicle and may present structural problems since it is near the normal load factor limit of 2.5 used by the Space Shuttle. The engine was flown at 100% power level from liftoff until the 3-g axial acceleration limit was reached at approximately125 sec into flight (h = 112 kft, M = 4.2). At this point the engine was gradually throttled down to nearly 20% at MECO to maintain the 3-g limit. The engine mixture ratio was varied continuously throughout ascent. The manner in which this parameter is varied during flight has a significant effect and will be discussed in more detail later.

<u>Structural Constraint</u>

One feature of the VentureStar™ design that could be exploited during ascent was its lifting body shape. By flying a lifting trajectory, it was possible to significantly decrease the amount of gravity losses, thereby improving vehicle performance and payload capability. Yet increasing the amount of lift during ascent generally required flight at higher angles-of-attack and resulted in greater stress on the vehicle structure. Accordingly, the nominal trajectory was constrained to keep the parameter q-α below a 1500 psf-deg structural design limit to ensure that the aerodynamic loads did not exceed the structural capability of the vehicle. The effect of this trajectory constraint on vehicle performance is shown in Fig. 3. There was a substantial benefit associated with using lift during ascent since flying a non-lifting trajectory resulted in a payload penalty of over 1000 lbs compared to the nominal case. As the q-α limit was raised the payload increased because the vehicle could use more lift to further reduce gravity losses. Eventually, the additional payload capability flattened out at a q-α limit near 5000 psf-deg because higher drag losses, which are also incurred by flying a lifting trajectory, began to overcome the corresponding decrease in gravity losses. The results shown in Fig. 3 only reflected the effect of changing the structural limit on vehicle performance and did not account for the impact of structural weight increases that would be required to design a vehicle that could endure higher aerodynamic loading.

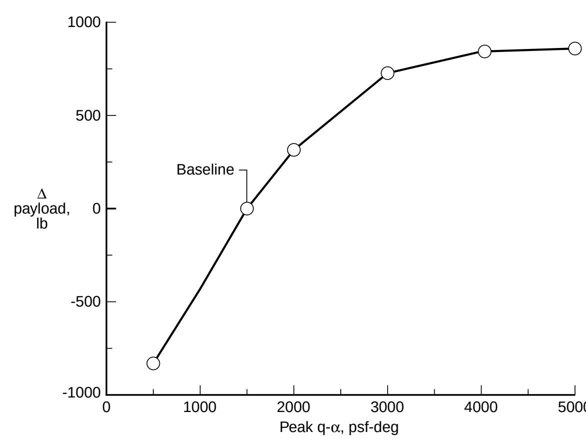

Figure 3. Effect of the q-α structural design constraint on vehicle payload capability.

<u>Axial Acceleration Limit</u>

A series of ascent trajectories was optimized at a range of axial acceleration constraints from 3 to 5-g's. Changing this constraint had a small effect on the vehicle payload capability (see Fig. 4). Increasing the acceleration limit from 3.0 to 3.3-g's resulted in slightly lower gravity losses, which led to an additional 300 lbs of payload capability. As the limit was increased beyond 3.3-g's, the lower gravity losses were eradicated by an increase in thrust vectoring losses (the ΔV required to turn the velocity vector). To insert into a 50 × 248 nmi-orbit, the vehicle must perform much of its pitch-over at altitudes high enough to avoid accumulating excessive drag losses. As the g-limit was increased, the velocity at which this pitch-over occurred became higher and more energy had to be expended to turn the velocity vector. Although changing the acceleration limit had a small effect on payload capability increasing the limit may be beneficial to the engine development since a higher limit enables higher power levels at MECO and shorter burn times (see Fig. 4). The former could facilitate the design of the engine control system while the latter may increase the overall engine life.

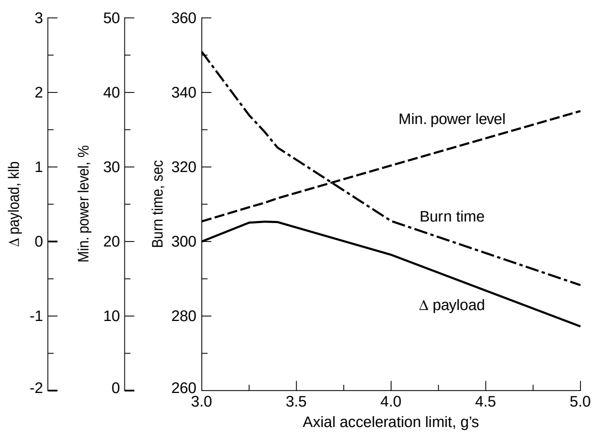

Figure 4. Effect of the axial acceleration limit on vehicle payload capability.

Pitch Trim Capability

The VentureStar™ is intended to be trimmed during ascent using only thrust vector control (TVC) supplied by the linear aerospike engine. The aerospike could produce a thrust moment to counteract the aerodynamic pitching moment of the vehicle by diverting up to 15% of the outflow from the top engine banks to the bottom engine banks, or vice-versa. Diverting the flow created a couple from the difference in axial force between the top and bottom of the engine (although the net axial force remained unchanged). This couple was the largest contributor to the total thrust moment (there was an additional smaller contributor due to differences in the normal force acting on the top and bottom engine ramps). An engine performance database created by LaRC that included TVC data was used to assess the impact of a trim constraint on the nominal ascent trajectory. The trimmed trajectory was designed such that no more than 50% of the control authority was used throughout the ascent. The vehicle cg was varied linearly with weight from the lift-off position of 39.9% of the reference length (nose to cowl) to the MECO value of 77.6%. In order to keep the amount of TVC used below 50%, the angle-of-attack had to be kept within the envelope shown in Fig. 5. Also shown in Fig. 5 are the angle-of-attack profiles for the trimmed and untrimmed nominal ascent trajectories. At altitudes below 40-kft, the angle-of-attack had to be kept lower than optimal in order to meet the trim constraint. This loss of optimality led to an 1100-lb penalty in vehicle payload capability. Note that the TVC effectiveness varied with altitude and was lowest at 35-kft where the angle-of-attack had to be kept within a 1.3° window.

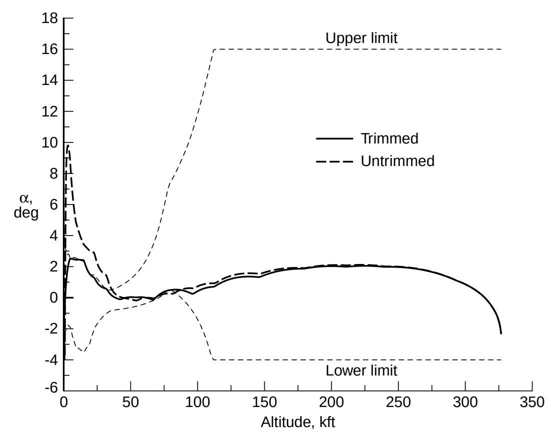

Figure 5. Effect of trim constraint on angle-of-attack profile for nominal ascent trajectory.

The baseline configuration discussed in this paper had the LOX tank positioned in the nose of the vehicle. One trade that was considered by the LaRC team was moving the LOX tank to the aft end of the vehicle which could potentially decrease the weight of the LH_2 tank and the intertank structure significantly. One concern with moving the LOX tank aft, however, was the effect of the resulting rearward shift in cg location on the ability of the vehicle to trim during ascent. The effect of pitch trim was computed for two LOX aft vehicles that were modeled as having a constant cg position during ascent at locations of 78% and 82% of the reference body length (nose to cowl), respectively. Figure 6 compares the trim capability of these LOX aft configurations with the baseline LOX forward configuration. These results show that the TVC requirements actually decreased the

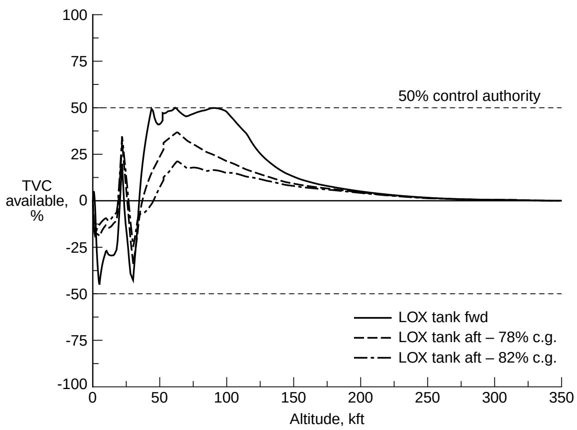

Figure 6. Comparison of the thrust vector control profile required for pitch trim for the baseline and two LOX-aft configurations.

more the longitudinal cg was moved aft. This behavior occurred because most of the thrust moment was due to the couple created by the difference in axial force between the top and bottom engine banks. Since this couple was independent of longitudinal cg position, the maximum attainable thrust moment did not change much as the cg was moved. The effect of the cg location was much stronger on the aerodynamic moment, and a rearward shift in cg generally resulted in smaller aerodynamic moments for the low angles-of-attack seen during ascent. Therefore, the net effect of moving the LOX tank aft was to increase the pitch trim control margin. Although moving the LOX tank aft may ease pitch trim concerns during ascent, more work must be done to fully understand the effect of such a move on pitch trim during entry.

Engine Performance Trades

With the aerospike engine it was possible to vary the mixture ratio between values of 5.5 and 7.0 during flight. In general, as the engine mixture ratio was increased, total thrust increased and the specific impulse (I_{SP}) decreased. Ideally the mixture ratio should be set high early in flight, where high thrust levels are required to accelerate the fuel-heavy vehicle, and later transitioned to the lowest allowable value to maximize vacuum I_{SP}. Generally engine development becomes more complicated and expensive as the flexibility of the engine to vary mixture ratio is increased.

A performance assessment was made for three different modes of mixture ratio adjustment during flight (constant, step, and continuously varying). In cases where the mixture ratio was varied, the total O/F ratio (the ratio of total LOX weight to total LH_2 weight) had to be kept consistent with the vehicle propellant tank design (baseline O/F was 6.0). The mixture ratio profiles for each case are shown in Fig. 7 along with the corresponding effect that each had on the I_{SP} profile. By continuously varying the mixture ratio, the inserted weight could be increased by 1900 lbs over the constant case and 200 lbs over the step case. In the step and variable cases the mixture ratio was initially set to 6.5 because the slight increase in thrust that could be gained by increasing the mixture ratio to 7.0 was overpowered by a greater loss in I_{SP}. The variable case differed from the step case at low altitudes because the mixture ratio profile could be tailored to take advantage of a lower I_{SP} caused by shock interference with the nozzle wall (see Reference 8). The profile differed at higher altitudes because it was more efficient to lower the thrust to meet the g-limit by decreasing mixture ratio (variable case) rather than power level (step case). The added design complexity of a continuously varying engine over one that performs a step change may not be worth the small accompanying performance increase.

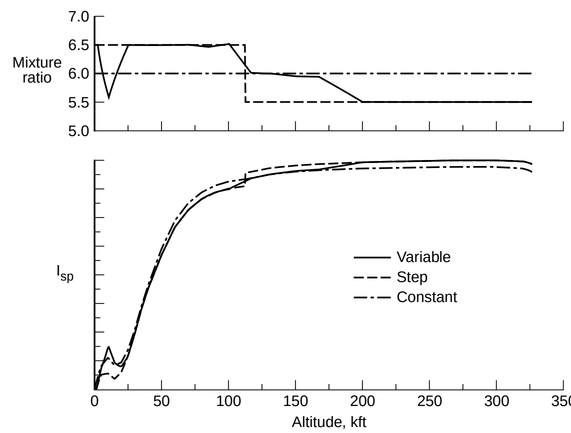

Figure 7. Engine mixture ratio profiles and corresponding effect on I_{SP} during flight.

Vehicle Sizing Studies

The liftoff T/W and total O/F ratios were critical parameters that influenced the weight and performance of the vehicle. Since both of these parameters affected weight and performance in opposite ways, it was important to link the weight estimation and trajectory optimization in order to capture the combined effect. An iterative process was undertaken that coupled the results of POST and CONSIZ. This process began with an initial guess of the mass ratio ($GLOW/W_{ins}$) which is a measure of vehicle performance. Next, values for the liftoff T/W and O/F ratio were selected. All three of these parameters were input into CONSIZ to determine their effect on the weight of the VentureStar™ vehicle. The mass ratio essentially determined the total propellant load of the vehicle. The liftoff T/W was directly proportional to the size of the engine and impacted the weight of the propulsion system (engines, feed system, etc) and thrust structure. The total O/F ratio determined the propellant bulk density and consequently affected the weight of the tanks and propellants.

In this analysis, CONSIZ was used to size the vehicle to deliver a 25,000-lb payload to the ISS. That is, as changes were made to mass ratio, liftoff T/W and the total O/F, the vehicle was photographically scaled to maintain a fixed 25,000-lb payload. Favorable changes to these three parameters resulted in a vehicle that was smaller than the baseline (in physical dimensions and empty weight) and could still deliver the required payload. The vehicle was scaled under the assumption that the volumetric efficiency (ratio of tank volume to total volume) remained constant. The impact of this assumption was not significant since vehicles were not scaled by huge amounts (less than 15% throughout the study) and the results were concerned primarily with changes in empty weight rather than absolute values. Using this technique the effect of the liftoff T/W and total O/F on the empty weight was determined with the assumption that a vehicle with a lower empty weight would ultimately have lower development costs.

The other key component of this iterative sizing process was the optimization of the ascent trajectory using the weights calculated with CONSIZ. The same mission and constraints listed in Table 1 were used in the trajectory calculations. For each optimized trajectory the engine performance model was scaled to meet the required liftoff T/W and the engine mixture ratio was varied such that the total O/F was consistent with what was used in the weight calculation. Trajectories were determined that maximized the weight inserted into orbit, (which was equivalent to the lowest possible mass ratio). Once the minimum mass ratio was determined from the trajectory optimization, it was fed back into CONSIZ and this whole process was repeated until convergence. This entire multidisciplinary analysis was performed for enough values of T/W and O/F to demonstrate how the empty weight changed with respect to the baseline vehicle.

The effect of the total O/F ratio on the empty weight is shown in Fig. 8. All values have been normalized with respect to the baseline vehicle (T/W = 1.35, O/F = 6.0). Changing the O/F ratio had a notable effect on empty weight and led to differences of more than 5% between the best and worst values. The optimal O/F value for a

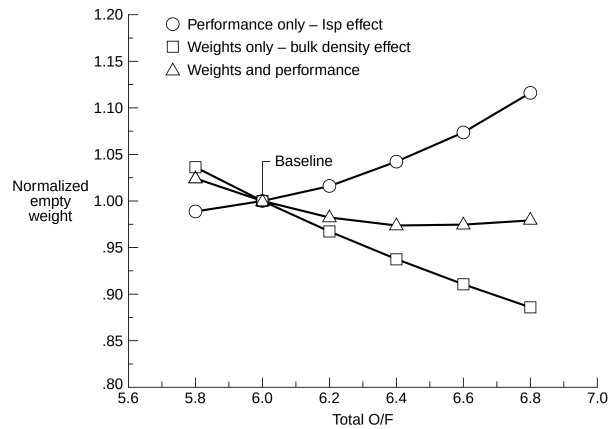

Figure 8. Variation of vehicle empty weight with total O/F ratio (normalized with baseline).

liftoff T/W of 1.35 was approximately 6.5 and was characterized by a reduction in empty weight of over 2.5% from the baseline. Two additional curves are shown in Fig. 8 to demonstrate the importance of coupling the performance and sizing analyses. When only performance changes due to varying the total O/F were considered (i.e., weight changes due to varying the propellant bulk density were neglected) the empty weight increased rapidly as the total O/F was raised. This increase occurred because the engine had to operate at high mixture ratios for a longer duration during the trajectory in order to raise the total O/F, thus decreasing the average I_{SP} and increasing the mass ratio. On the other hand, if the mass ratio was assumed to remain constant as the total O/F ratio was changed (i.e., the effect of total O/F on performance was neglected) then the empty weight went down as the total O/F was increased. This improvement in empty weight occurred because of the increase in propellant bulk density resulting from the higher ratio of liquid oxygen to liquid hydrogen. With a larger bulk density, more propellant could be held in a given volume, so that, with no penalty in performance, a smaller vehicle could carry the same amount of propellant and consequently deliver the same payload to the target orbit. In reality, both effects work against each other, resulting in the actual curve that was minimized around 6.5. This trend was nearly independent of the liftoff T/W, with the optimal ratio of LOX to LH_2 weight being around 6.5 for values of liftoff T/W between 1.15 and 1.35 (see Fig. 9).

A similar trade was conducted to determine the sensitivity of empty weight to liftoff T/W. The results of this trade assuming a total O/F ratio of 6.0 are presented in Figure 10. Each point on the curve was determined using the same iterative process that was used in the O/F trade. The empty weight was minimized when the lift-

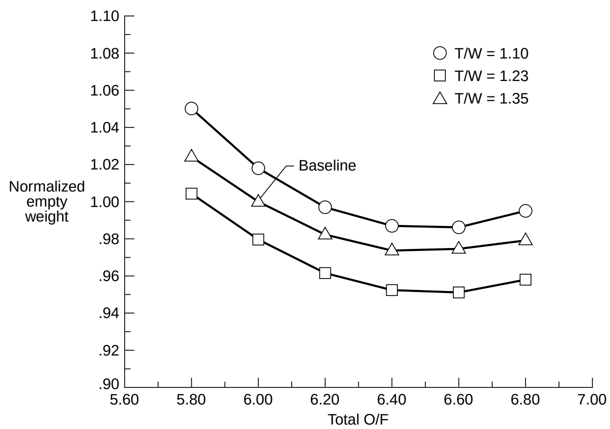

Figure 9. Effect of liftoff T/W on optimal O/F ratio.

off T/W was approximately 1.23. Changing the T/W from 1.35 (baseline) to 1.23 resulted in a 2% decrease in empty weight. If gross lift-off weight was minimized instead of empty weight (also shown in Fig. 10), the optimal T/W was somewhat higher (between 1.30 and 1.35). The optimal T/W differed between the two curves because the increase in engine weight that would accompany a higher liftoff T/W was a much larger percentage of empty weight than GLOW. Therefore the performance benefit from a higher T/W was overcome by the added engine weight sooner when empty weight was minimized. Since cost is more closely related to the empty weight rather than GLOW, the lower T/W of 1.23 would likely lead to the lower cost configuration. However, the benefit in empty weight resulting from a lower T/W would have to be weighed against the affect such a change might have on the engine-out abort capability of the vehicle. For VentureStar™ in particular, a single engine-out is

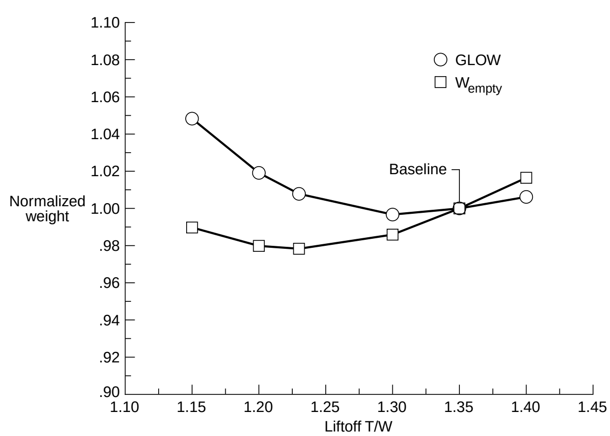

Figure 10. Variation of gross liftoff weight and vehicle empty weight with liftoff T/W ratio (normalized with baseline).

actually two engines-out (an additional engine must be powered down to eliminate thrust imbalances between each side of the linear aerospike). This would limit the lower T/W bound to about 1.25 assuming a 10% throttle up of the remaining engines.

The trend of empty weight with liftoff T/W was independent of the total ratio of LOX to LH2, with the optimal T/W being about 1.23 for O/F ratios between 6.0 and 6.5 (see Fig. 11). As shown in the figure, a 5% decrease in empty weight is possible by changing the baseline values of liftoff T/W from 1.35 to 1.23 and total O/F from 6.0 to 6.5, abort concerns notwithstanding. Also shown in Fig. 11 is the influence of the weight of the engine per pound of thrust (engine T/W) on the optimal value of liftoff T/W. The engine T/W is a key input to the weights model and directly influences the weight of a number of propulsion system elements. For a decrease in engine T/W of 10%, the trend of empty weight with respect to lift-off T/W was unchanged, although the empty weight increased uniformly by over 6%.

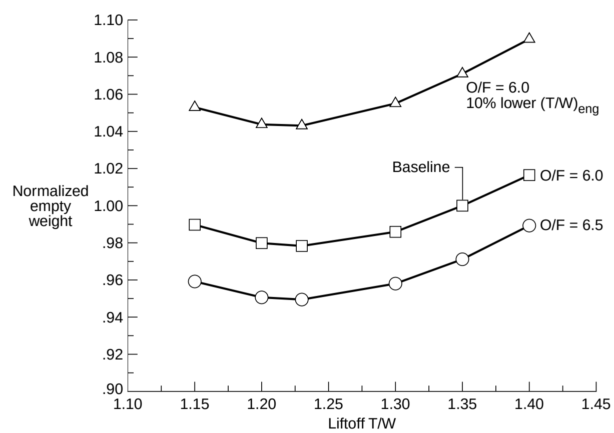

Figure 11. Effect of O/F ratio and engine T/W on optimal liftoff T/W.

Entry Trajectory Performance

An aerospace vehicle that operates in the hypersonic flight regime must be protected from the aerodynamic heating environment. The use of a relatively low-temperature (~1800°F max) metallic thermal protection system has been proposed to meet this need for the VentureStar™ RLV. In contrast, the current Shuttle orbiter employs relatively high-temperature ceramic tiles (~2600°F max). Although the metallic system may offer some benefit in reduced maintenance requirements, its lower temperature capability necessarily constrains the vehicle flight envelope so that excessive heating levels are avoided. The lowest achievable peak laminar heating rate is a function of the vehicle configuration, hypersonic aerodynamics, and weight (W/C_LS).[13] Based on the preliminary assessment shown in Fig. 12, it appeared possible, in theory, to maintain the VentureStar™ laminar heating levels to within the limits required for the metallic TPS. However, turbulent heating levels can easily double the laminar values. Reference 14 illustrates the dramatic impact transition can have on TPS requirements, particularly in the case of a metallic system.

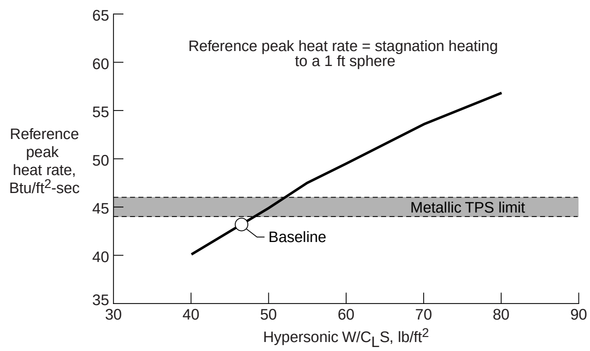

Figure 12. Variation of peak reference heating rate with W/C_L-S.

The objective of the entry trajectory development was to limit the laminar heating to levels within the capability of the proposed TPS and to delay the onset of transition such that turbulent heating levels did not exceed those experienced in the earlier laminar phase of the entry. A coupled approach that used POST and MINIVER together was employed to achieve these heating objectives and to satisfy other flight constraints such as the minimum crossrange requirement (750 nmi). Initially, a two-phased approach was used to develop an entry trajectory that met the thermal constraints. In the first phase, aerothermal constraints were imposed on the entry through the use of a reference heating indicator based on the work of Chapman.[15] This correlation, as applied in POST, is roughly proportional to $\rho^{1/2}v^3$. Although it is only an indicator of stagnation heating rates and loads, windward areas of the vehicle (where laminar continuum flow predominates) typically tend to track this indicator. Thus, it can be used directly in the optimization process if the appropriate target value can be determined. For this investigation it was assumed that keeping the chine and nosecap regions below radiation equilibrium temperatures of 2000°F, was sufficient to limit most of the acreage to temperatures below the 1800°F allowable for the metallic TPS. Heat transfer distributions for the similarly shaped X-33 vehicle supported this assumption.[16] Transforming the temperature limit (2000°F) to a heating rate, adjusting for the vehicle scale and applying a hot-wall correction resulted in the desired reference heating rate for the trajectory optimization process. This value (~45 Btu/ft^2-sec) was very close to the theoretical minimum noted in Fig. 12.

Once a trajectory that met the laminar heating constraint was computed, the trajectory was post-processed using MINIVER to determine the occurrence of transition and the expected laminar and turbulent heating levels at the vehicle surface. The thermal model used in MINIVER was the same as that used in Reference 11 which was shown to yield excellent agreement with detailed CFD predictions obtained for a similar lifting body configuration. The parameter used to predict transition onset in this study, Re_θ/M_e, is one which has been extensively validated in the Shuttle program.[17] Unlike a simple length-based Reynolds number, this local parameter takes into account angle-of-attack effects, known to have a strong influence on the occurrence of transition. The transition work of Thompson, et al presented in Reference 18, led to selection of a value of 250 for this study. In Thompson's paper, this parameter was predicted using the inviscid/boundary-layer code LATCH[19] and compared to experimental observations of transition on the X-33 forebody. A value of 300 was found to accurately predict smooth-body transition results. Potential roughness elements on the metallic TPS led to the selection of the more conservative value of 250 for the work presented here.

An evaluation of the initial entry trajectory that was post-processed using MINIVER indicated acceptable laminar but excessive turbulent heating rates. The high turbulent heating rates occurred because the optimized trajectory required flight at altitudes low enough to induce transition between 10 and 15 kft/sec, where laminar heating rates were still fairly high. The flight profile was optimized at these lower altitudes because the density was higher and more lift could be generated to help meet the 750 nmi minimum crossrange requirement. This two-phase approach, in which a trajectory was first developed based on laminar heating constraints and then post-processed to evaluate for transitional heating levels, was found to be cumbersome and failed to take advantage of the optimization capability within POST. An alternative approach was taken that indirectly coupled POST and MINIVER so that the transition parameter Re_θ/M_e could be used to influence the trajectory design. A series of MINIVER solutions were generated at a reference point immediately ahead of the expansion on the windward surface (90% of the vehicle length) for a range of velocities from 5 to 17 kft/sec and angles of attack from 20° to 50°. For each angle of attack and velocity, the altitude at which the transition parameter (Re_θ/M_e) reached a pre-selected value was determined. Tables rep-

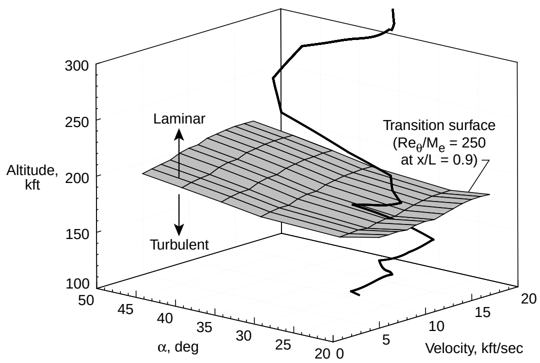

Figure 13. Optimized entry trajectory and transition constraint surface.

resenting a series of "transition surfaces" similar to the one shown in Fig. 13 were generated for transition parameter values ranging from 200 to 350. These tables were used to place additional constraints on the trajectory optimization in order to delay transition to as low a Mach number as possible.

The success of this approach depended on the ability of MINIVER to accurately predict the transition parameter Re_θ/M_e. This capability is demonstrated in Fig. 14 where LATCH-based predictions were compared to predictions made using MINIVER. This comparison is illustrative of the level of agreement between MINIVER and LATCH windward centerline predictions for VentureStar™ and the subscale X-33 demonstrator. Similar agreement was obtained for five other representative flight conditions ranging from Mach 10 to 20 and five angles of attack from 25° to 45°.

Using the existing reference heating calculation together with the new transition tables, an optimized entry trajectory which targeted the desired heating rates and loads was generated for the VentureStar™. Simultaneously the onset of transition to turbulent flow was delayed. This optimized entry trajectory is presented in Fig. 15. The trajectory began with a deorbit maneuver from the ISS orbit that put the vehicle at atmospheric interface (altitude of 400 kft) with a flight path angle of –1.1°. At this point the angle-of-attack and bank angle profiles were tailored to minimize the reference heating rate and to meet the 750 nmi minimum crossrange requirement. In addition, the effect of trimming the vehicle in pitch using body flap and elevon deflections was modeled, and constraints were placed on the trajectory to ensure that the control surface deflections required for trim remained below 20°. Also, for this trajectory transition was delayed to approximately Mach 9.3. To delay transition for as long as possible, the vehicle flew near the transition surface (see Fig. 13) beginning at a velocity of approximately 12 kft/sec until transition finally occurred near 10 kft/sec. Subsequent heating predictions based both on MINIVER and more detailed solutions using

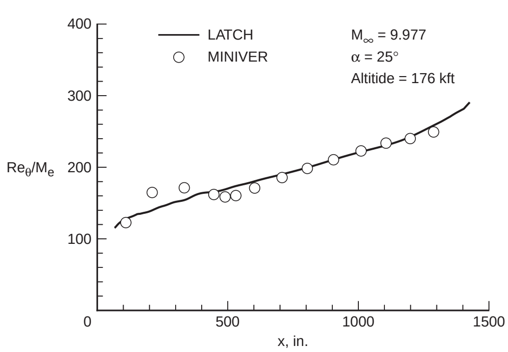

Figure 14. MINIVER/LATCH Re_θ/M_e centerline comparison.

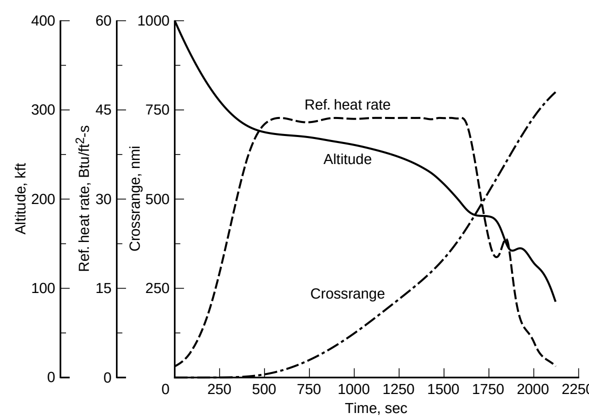

Figure 15. Altitude, reference heating rate and crossrange profiles for optimized nominal entry trajectory.

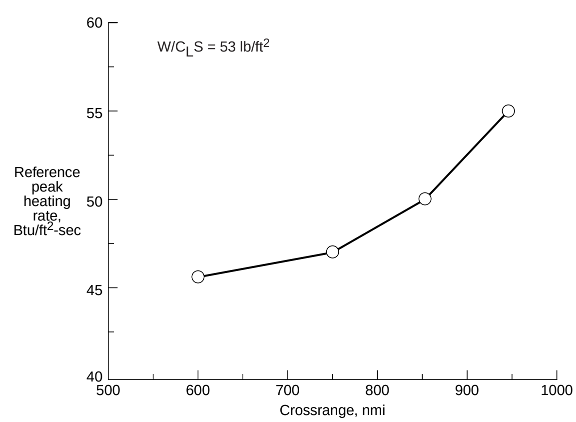

Figure 16. Effect of minimum crossrange requirement on reference peak heating rate.

LATCH, indicated that peak laminar and turbulent heating levels were indeed within the capability of the metallic TPS. Figure 16 shows the effect of the crossrange requirement on the minimum peak heating rate for a typical lifting body configuration. As shown, lowering the 750 nmi requirement would not enable significantly lower peak heating rates.

The transition surfaces generated for this study cannot be applied directly to other configurations. However, the procedure to develop similar transition surfaces is straightforward. MINIVER has been successfully used to predict the windward centerline heating environments for a wide variety of configurations. Assuming that a reasonable assumption can be made for the transition value of Re_θ/M_e, surfaces similar to those developed here can be generated rapidly to aid in the trajectory development process for other vehicles. The integration of the aerothermal/TPS considerations directly within the trajectory optimization as developed here can potentially reduce the number of design cycles required to achieve the optimal trajectory/TPS balance for hypersonic flight vehicles.

SUMMARY

Lockheed Martin Skunk Works is currently developing a single-stage-to-orbit reusable launch vehicle called VentureStar™. As part of the X-33 program, NASA Langley Research Center participated in conceptual studies that focused on the design, analysis and screening of a number of early VentureStar™ concepts and configurations. This investigation presents the results of various performance trade studies that were performed in support of this effort. These trade studies were conducted using a multidisciplinary performance analysis approach that indirectly coupled trajectory optimization, weight estimation and heating analysis tools.

The sensitivity of vehicle performance to a number of ascent trajectory constraints was determined. Results were presented that quantified the benefit of utilizing the VentureStar™ shape to fly a lifting trajectory. Although the flight profile had to be limited so that structural design limits were not exceeded, using lift during ascent still resulted in additional payload capability of over 1000 lbs. In addition it was found that the axial acceleration limit did not have a significant effect on payload capability, although altering it may ease engine-operating requirements. Finally, requiring the vehicle to be trimmed in pitch during ascent limited the range of angles-of-attack that could be flown and resulted in a payload penalty of more than 1000 lbs compared to an untrimmed case where this requirement was ignored. Also, the pitch trim control authority of the linear aerospike thrust vector control system was relatively independent of longitudinal cg location. This insensitivity to cg location may be advantageous for a configuration with the liquid oxygen tank located in the aft end of the vehicle.

The linear aerospike engine had the ability to vary the mixture ratio during flight. Varying the mixture ratio in a step-like or continuous manner throughout the ascent increased the vehicle payload capability by nearly 2000 lbs compared to the case in which it was held constant. Also, by varying the mixture ratio profile, the total oxidizer to fuel ratio of the vehicle could be affected. Since this ratio influenced the weight and performance of the vehicle, its true effect could only be determined through an approach that coupled the vehicle sizing with the trajectory optimization. This approach was also used to determine the optimal liftoff thrust-to-weight ratio which was directly related to the size of the engine. By changing the oxidizer-to-fuel ratio to 6.5 and the liftoff thrust-to-weight ratio to 1.23, the vehicle empty weight could be reduced by 5% compared to the baseline case.

In addition to the ascent trajectory trades, coupled trajectory/thermal analyses were conducted to optimize the VentureStar™ entry flight profile to the requirements of its proposed metallic thermal protection system. The objective of these analyses was to limit the laminar heating to levels within the capability of the proposed TPS and to delay the onset of transition such that turbulent heating levels did not exceed those experienced in the earlier laminar phase of the entry. Using an aerothermal analysis tool, transition surfaces were generated that could be used to predict transition onset as a function of altitude, velocity and angle-of-attack. These surfaces were used directly by the trajectory optimization tool to achieve the heating objectives while meeting the minimum crossrange requirement of 750 nmi. Reducing the crossrange requirement did not result in significantly lower peak heating rates.

This study provided a broad view of a number of issues and concerns that should be considered in the performance analysis of a lifting body single-stage-to-orbit RLV. Emphasis was placed on the multidisciplinary nature of the analyses that were performed. It was necessary to couple the trajectory optimization with other discipline tools since changes in vehicle performance often affected the weight and design of many different systems. Capturing the effect of various design changes on both weight and performance is vital if the physical difficulty and small margins that characterize the design of a fully reusable single-stage launch vehicle are to be overcome.

ACKNOWLEDGEMENTS

The authors would like to acknowledge Lockheed Martin Skunk Works for the opportunity to work with them on VentureStar™ and for the various data models that were provided by them during the course of this analysis. In addition, the authors would like to thank Anne Costa who was instrumental in the preparation of this paper for publication.

REFERENCES

1. Stanley, D.O., Engelund, W.C., Lepsch, R.A., McMillin, M., Wurster, K.E., and Powell, R.W., "Rocket-Powered Single-Stage Vehicle Configuration Selection and Design," AIAA Paper 93-1053, Feb. 1993.

2. Stanley, D.O., Engelund, W.C., and Lepsch, R.A., "Propulsion System Requirements for Reusable Single-Stage-to-Orbit Rocket Vehicles," AIAA Paper 92-3504, July 1992.

3. Access to Space Advanced Technology Team Final Report. NASA Langley Research Center, Vol. 3, Design Data, July 1993.

4. Baumgartner, R. I. and Elvin, J. D., "Lifting Body – An Innovative RLV Concept," AIAA Paper 95-3531, Sept. 1995.

5. Lockwood, M. K., "Overview of Conceptual Design of Early VentureStar Configurations," AIAA Paper 2000-1042, Jan. 2000.

6. Brauer, G. l., Cornick, D. E., and Stevenson, T., "Capabilities and Applications of the Program to Optimize Simulated Trajectories (POST)," NASA CR-2770, Feb. 1977.

7. Lepsch, R.A., Stanley, D.O., and Unal, Resit, "Application of Dual-Fuel Propulsion to a Single Stage AMLS Vehicle," AIAA Paper 93-2275, June 1993.

8. Korte, J., "Parametric Model of An Aerospike Rocket Engine," AIAA Paper 2000-1044, Jan. 2000.

9. Engel, C. D. and Praharaj, S. C., "MINIVER Upgrade for the AVID System, Vol. I: LANMIN User's Manual," NASA CR-172212, Aug. 1983.

10. Wurster, K. E., Riley, C. J., and Zoby, E. V., "Engineeering Aerothermal Analysis for X-34 Thermal Protection System Design," *Journal of Spacecraft and Rockets*, Vol. 36, No. 2, 1999, pp. 216-228.

11. Gnoffo, P. A., Wurster, K. E., Bibb, K. L., and Mitcheltree, R. A., "Summary of Phase I Computational Aerothermodynamic Support for the X33 Lockheed Team," 1996.

12. Wurster, K. E. and Stone, H. W., "Aerodynamic Heating Environment Definition/Thermal Protection System Selection for the HL-20," *Journal of Spacecraft and Rockets*, Vol. 30, No. 5, 1993, pp. 549-557.

13. Wurster, K. E. and Eldred, C. H., "Technology and Operational Considerations for Low-Heat-Rate Trajectories," *Journal of Spacecraft and Rockets*, Vol. 17, No. 5, 1980, pp. 459-464.

14. Wurster, K. E., "An Assessment of the Impact of Transition on Advanced Winged Entry Vehicle Thermal Protection System Mass," AIAA Paper 81-1090, June 1981.

15. Chapman, D. R., "An Approximate Analytical Method for Studying Entry into Planetary Atmospheres," NASA TR R-11, 1959.

16. Hamilton, H. H., II, Weilmuenster, K. J., Horvath, T. J., and Berry, S. A., "Computational/Experimental Aeroheating Predictions for X-33 Phase II Vehicle," AIAA Paper 98-0869, Jan. 1998.

17. Bouslog, S. A., An, M. Y., and Derry, S. M., "Orbiter Windward-Surface Boundary-Layer Transition Flight Data," in Orbiter Experiment (OEX) Aerothermodynamic Symposium: Part 2, Throckmorton, D. A., ed., NASA CP-3248, pp. 703-740.

18. Thompson, R.A., Hamilton, H.H., II, Berry, S.A., Horvath, T.J., and Nowak, R.J., "Hypersonic Boundary-Layer Transition for X-33 Phase 2 Vehicle," NASA/TM-1998-207316, 1998.

19. Hamilton, H. H., II, Greene, F. A., and DeJarnette, F. R., "Approximate Method for Calculating Heating Rates on Three-Dimensional Vehicles," *Journal of Spacecraft and Rockets*, Vol. 31, No. 3, 1994, pp. 345-354.